Chapter 1

Large Blood Vessels

1.1   Introduction — The Cardiovascular System

The heart is a pump that circulates blood to the lungs for oxygenation (pulmonary circulation) and then throughout the systemic arterial system with a total cycle time of about one minute. From the left ventricle of the heart, blood is pumped into the aorta, which in adult humans has a diameter of about 2.5 cm and has a complex three-dimensional geometry. The three coronary arteries branch directly off the aorta to supply the heart. Daughter arteries branch directly from the aorta with further divisions ultimately down to the smallest blood vessels, the capillaries, in which the main exchange processes between the blood and tissues take place.

The blood returns via venules through a converging system of veins.

(i) <u>Arteries</u>

The walls of the arteries have a three-layer structure made of similar materials but in different proportions resulting in different mechanical properties (Figure 1.1).
I. The intima — lined with a single layer of cells called the endothelium, where atherosclerotic plaques first develop.

II. The media — consists of multiple layers of an elastic material, elastin, whose direction changes radially, separated by thin layers of connective tissue, collagen, with a few muscle cells.
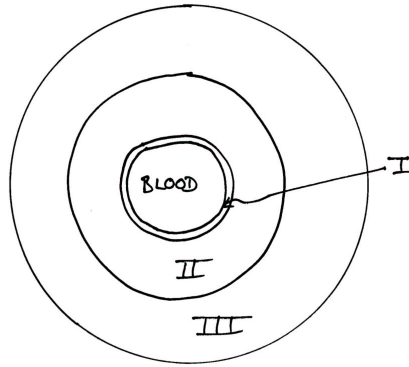
Figure 1.1: Structure of the arterial wall

III. The adventitia — loose connective tissue of elastin and collagen fibres.

The media is structurally most important and renders the arteries to be pre-stressed, non-linearly elastic tubes.

(ii) <u>Blood</u> — consists of cells in plasma,

$$\mu_p \approx 1.2\text{---}1.6 \times 10^{-3}\,\mathrm{kg\,m^{-1}\,s^{-1}}.$$

<u>Red Blood Cells</u> — 45% by volume.

Biconcave discs, very deformable with viscous contents (Figure 1.2). They may aggregate.
<u>Viscosity</u>

For shear rates $> 100\,\mathrm{s^{-1}}$, the fluid is approximately Newtonian:

$$\mu \approx 4 \times 10^{-3}\,\mathrm{kg\,m^{-1}\,s^{-1}} \quad \text{at} \quad 37^{\circ}\mathrm{C}$$

$$\rho \approx 1.05 \times 10^{3}\,\mathrm{kg\,m^{-3}}.$$

In the arteries and veins, with diameters $> 100\,\mu\mathrm{m}$, blood can be treated as homogeneous and Newtonian.
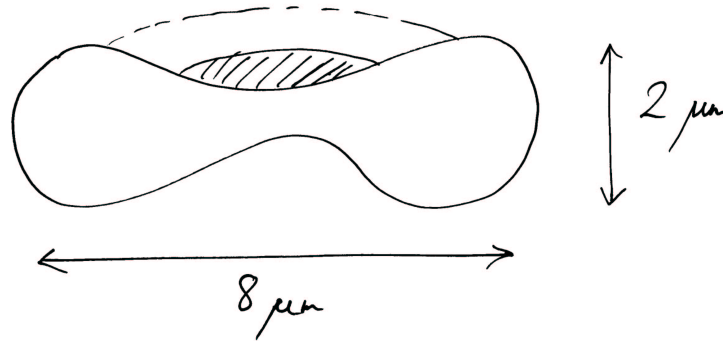
Figure 1.2: A red blood cell

1.2 One-dimensional theory of pulse propagation in arteries

.

Want to explain the mechanism and speed of propagation, changes in the shape of the pressure waveform (peaking and steepening downstream) and of the velocity waveform.

Consider an infinitely long, distensible tube of uniform undisturbed area, A_0, containing an incompressible, inviscid fluid of density, ρ.

Assume the wavelengths of the disturbances $\gg$ diameter of the tube

$\Longrightarrow$ velocity profile is flat and lateral velocities can be neglected (Figures 1.3 and 1.4).

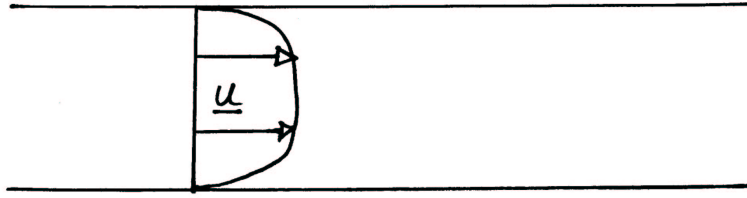| Variables:	excess pressure	$p(x,t)$
	area	$A(x,t)$
	averaged fluid velocity	$u(x,t)\mathbf{i}$.

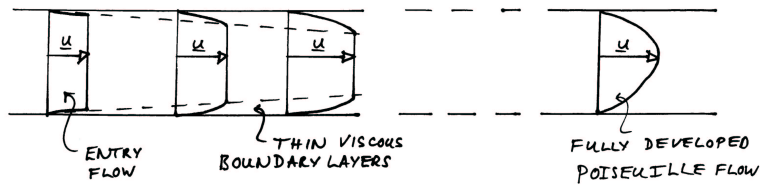Figure 1.3: Observed velocity profiles are flat, entry-type flows.

Figure 1.4: Development of entry flow.

1.2.1   Conservation of Mass

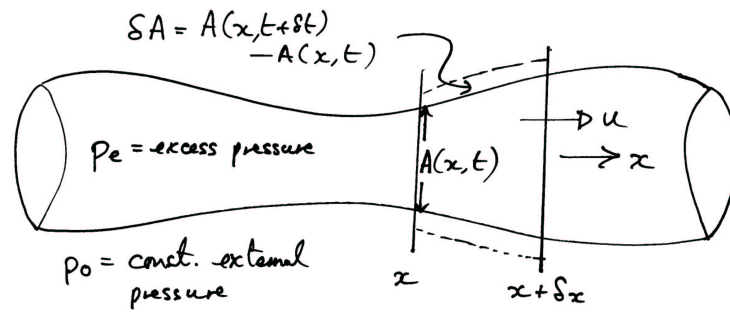Consider a small region of the pipe between x and $x + \delta x$ (Figure 1.5). In

Figure 1.5: Conservation of mass sketch.

time δt, the net flux into the region is approximately

$$\rho\left[\left(uA\right)|_x - \left(uA\right)|_{x+\delta x}\right]\delta t$$

and the resulting change in mass is approximately

$$\rho\left[A\left(x, t + \delta t\right) - A\left(x, t\right)\right]\delta x.$$

Equating these gives

$$\frac{(uA)\mid_x - (uA)\mid_{x+\delta x}}{\delta x} = \frac{A(x, t+\delta t) - A(x,t)}{\delta t},$$

and, as $\delta t, \delta x \longrightarrow 0$, we get

$$\frac{\partial A}{\partial t} + \frac{\partial}{\partial x}(uA) = 0. \tag{1.1}$$

1.2.2   Conservation of Momentum

Directly from the Navier-Stokes equations on setting $\mathbf{u} = u(x,t)\mathbf{i}$ and $Re = \infty$, we have

$$\frac{\partial u}{\partial t} + u\frac{\partial u}{\partial x} + \frac{1}{\rho}\frac{\partial p}{\partial x} = 0. \tag{1.2}$$

1.2.3   Constitutive Relation

$$p \equiv p_e - p_0 = P(A) = \text{transmural pressure} \tag{1.3}$$

i.e. pressure is a function of the cross-sectional area.

1.2.4   Linear Theory

For small amplitude disturbances, let

$$A = A_0 + a, \quad |a| \ll A_0, \quad |u| \ll 1$$

and note that from (1.3)

$$\frac{\partial p}{\partial t} = P'(A_0)\frac{\partial a}{\partial t} + 0(a^2).$$

Equations (1.1) and (1.2) give

$$\left.\begin{array}{ll} \dfrac{1}{A_0 P'(A_0)} \ \dfrac{\partial p}{\partial t} + \dfrac{\partial u}{\partial x} = 0 \\[2mm] \dfrac{\partial u}{\partial t} + \dfrac{1}{\rho}\dfrac{\partial p}{\partial x} = 0 \end{array}\right\} \tag{1.4}$$

on neglecting small quantities. Eliminating u gives

$$\frac{\partial^2 p}{\partial t^2} = c_0^2 \frac{\partial^2 p}{\partial x^2}, \tag{1.5}$$

where

$$c_0^2 = (\rho D_0)^{-1} \tag{1.6}$$

and

$$\frac{d}{dp}\left(\frac{a}{A_0}\right) = \frac{1}{D_0}$$

or equivalently

$$D_0 = \frac{1}{A_0 P'(A_0)} \tag{1.7}$$

is the distensibility of the tube. Equation (1.5) is the wave equation and has solutions

$$\left. \begin{array}{rcl} p & = & f\left(x \pm c_0 t\right), \\ \text{with} \quad u & = & \mp \left(\rho c_0\right)^{-1} f\left(x \pm c_0 t\right), \\ a & = & A_0 \left(\rho c_0^2\right)^{-1} f\left(x \pm c_0 t\right) \end{array} \right\} \tag{1.8}$$

representing waves propagating with speed c_0. This linearisation is valid provided $\mid u \mid \ll c_0$.

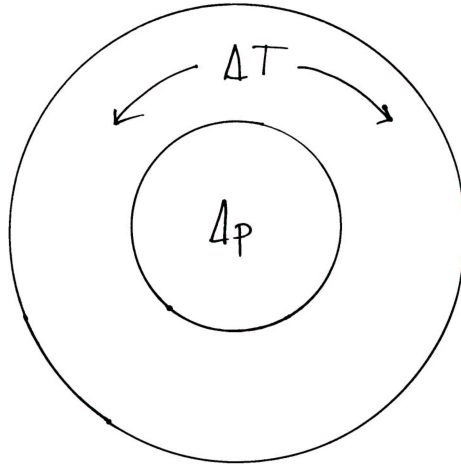c_0 can be estimated from values of Young's modulus, E, for arteries (Figure 1.6).

Figure 1.6: Idea: increase in pressure $\triangle p$ leads to increase in hoop tension $\triangle T$.

(Effective, incremental) Young's modulus (see Figure 1.7):

$$\delta T = Eh\frac{\delta \ell}{\ell} + O\left(\delta h \frac{\delta \ell}{\ell}\right)$$

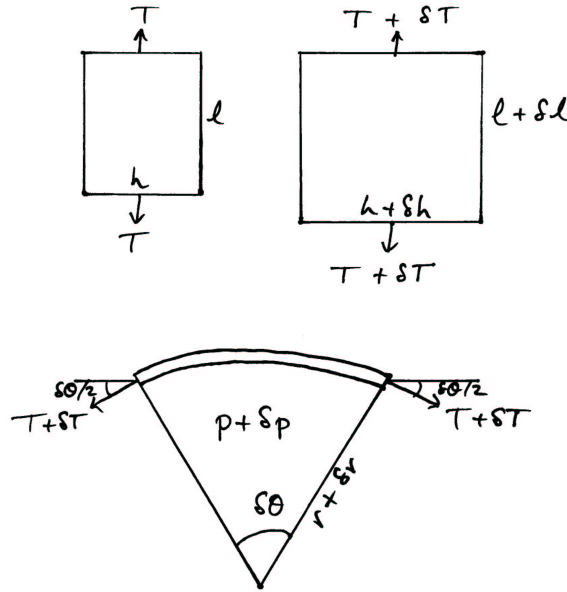Resolving radially (per unit length) over angle $\delta\theta$,

Figure 1.7: Definition sketch for Young's modulus.

$$2\,\delta T \sin(\delta\theta/2) \approx \delta T\,\delta\theta \approx \delta p(r\delta\theta) \quad\Longrightarrow\quad \delta T = r\delta p. \qquad (1.9)$$

$$\therefore \quad \delta T \;=\; Eh\frac{\delta\ell}{\ell} = Eh\frac{\delta r}{r} \quad (\Longleftarrow \ell = r\delta\theta)$$
$$=\; \frac{Eh}{2}\frac{\delta A}{A} \quad \text{since} \quad \left(A = \pi r^2 \Longrightarrow \frac{\delta A}{A} = \frac{2\pi r\delta r}{\pi r^2} = \frac{2\delta r}{r}\right).$$
$$(1.10)$$

From equations (1.6) and (1.7),

$$c_0^2 = \frac{A_0 P'(A_0)}{\rho} = \frac{A_0}{\rho}\frac{\delta p}{\delta A}$$

and, using (1.9) and (1.10), we see that

$$c_0^2 = Eh/2\rho r_0, \qquad (1.11)$$

where r_0 is the mean radius of the tube. This is the Moens-Korteweg wave speed (1878), although first discovered by Young in (1809).

c_0 as calculated from (1.11) is quite accurate predicting that $c_0 \approx 5\,\mathrm{m\,s}^{-1}$ in the human thoracic aorta and increases to about $8\,\mathrm{m\,s}^{-1}$ in the large peripheral arteries. However, refinements of the elastic theory to include longitudinal stresses and dynamic elastic properties increase c_0 by about 25% worsening the agreement with experiments.

Also equations (1.8) predict that the velocity and pressure wave forms will be the same and propagate without change of shape, in contradiction to the following observations, so other effects need to be included.

1.2.5   Observations

1. Velocity wave form different from pressure wave form.
   - Use viscous fluid theory in a rigid tube and can successfully predict velocity wave form from pressure wave form.

2. Peaking of pressure wave.
   - Explained by reflections.

3. Attenuation (experiments at high frequency)
   - need viscoelastic effects to model successfully, viscous fluid is insufficient.

1.3 Wave reflections

The aim is to explain the peaking of the pressure pulse (see Figure 1.8).

We begin by analysing the reflection and transmission of a wave at an
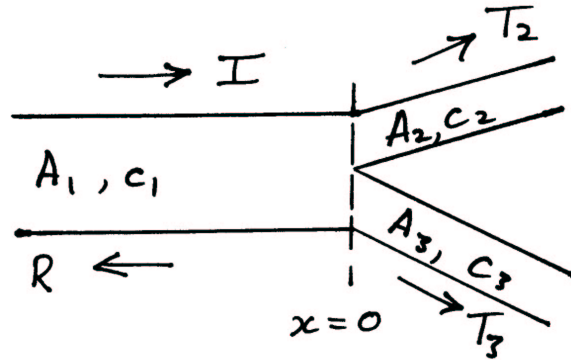

Figure 1.8: Wave reflection at a bifurcation. I = incident wave. R = reflected wave. T = transmitted wave. A = cross-sectional area. c = wave-speed.

isolated bifurcation.

The incident pressure wave is $p_I = P_I f(t - x/c_1)$. P_I is the amplitude, f is the wave form.

The flow rate associated with the incident wave is $A_1 u_I$ which equals

$$Q_I = Y_1 P_I f(t - x/c_1),$$

where $Y_1 = A_1/\rho c_1$ from (1.8), is the characteristic admittance. (Here A_1 is the undisturbed area and we have neglected the perturbation, a.)

The reflected wave has pressure

$$p_R = P_R \ g(t + x/c_1)$$

and flow

$$Q_R = -Y_1 \ P_R \ g(t + x/c_1),$$

and, for the transmitted waves,

$$p_j = P_j h_j(t - x/c_j), \quad Q_j = Y_j P_j h_j(t - x/c_j),$$

where

$$Y_j = A_j/\rho c_j \qquad (j = 2, 3).$$

We need to match the pressure and the flow rate at the bifurcation at all times at $x = 0$.

$$\implies \quad g(t) = h_j(t) = f(t), \quad P_I + P_R = P_2 = P_3, \quad \text{and} \quad Y_1(P_I - P_R) = Y_2 P_2 + Y_3 P_3$$

$$\implies \quad \frac{P_R}{P_I} = \frac{Y_1 - (Y_2 + Y_3)}{Y_1 + (Y_2 + Y_3)} \qquad (1.12)$$

and

$$\frac{P_2}{P_I} = \frac{P_3}{P_I} = \frac{2Y_1}{Y_1 + (Y_2 + Y_3)}. \qquad (1.13)$$

Notes:

1. If $Y_2 + Y_3 < Y_1$, then the reflected pressure wave is in phase with the incident wave at $x = 0$ and the combined amplitude $P_I + P_R$ is greater than P_I alone. This is a "closed end" type of junction.

2. If $Y_2 + Y_3 > Y_1$, P_R is of opposite phase and the combined amplitude $P_I - P_R$ is less than P_I alone. This is an "open end" junction.

3. If $Y_2 + Y_3 = Y_1$, $P_R = 0$, there is no reflection and the junction is well-matched.

4. Most cardio-vascular junctions are well-matched except, notably in man, the iliac bifurcation which is of the closed-end type. This is certainly a contributing factor to the peaking of the pressure pulse, although taper is also important.

1.4 Effect of viscosity - Womersley's Problem

We'll examine the effect of viscosity on a flow driven by an oscillatory pressure gradient in a rigid tube. The assumption of a rigid tube is OK because the distance travelled by a fluid element in 1 cycle $\ll$ wavelength and thus the tube is approximately parallel-sided (see Figure 1.9).
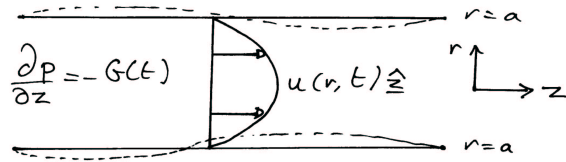

Figure 1.9: Wormersley's problem.

The pressure gradient is given as a Fourier expansion in t:

$$\frac{\partial p}{\partial z} = -\Re\left\{\sum_{n=0}^{\infty} G_n e^{in\omega t}\right\}. \tag{1.14}$$

$4 — 6$ modes are usually sufficient to model the pressure pulse and about 10 modes suffice for the velocity wave form.

The z-component for the Navier–Stokes equations in cylindrical polar coordinates gives

$$u_t = -\frac{p_z}{\rho} + \frac{\mu}{\rho}\left(u_{rr} + \frac{1}{r}u_r\right) \tag{1.15}$$

$$\text{with b.c.'s} \quad \left.\begin{array}{ll} u = 0 & \text{on} \quad r = a, \\ u_r = 0 & \text{on} \quad r = 0. \end{array}\right\} \tag{1.16}$$

Suppose that the Fourier series for $u(r,t)$ is

$$u = u_0(r) + \sum_{n=1}^{\infty} u_n(r)e^{in\omega t}. \tag{1.17}$$

Substitute into (1.15) and solve the linear ODE's term by term.
The fundamental mean flow is

$$u_0(r) = \frac{G_0 a^2}{4\mu}\left(1 - \frac{r^2}{a^2}\right) \quad — \quad \text{Poiseuille flow.} \tag{1.18}$$

The oscillatory terms come from solutions of Bessel's Equation *(Exercise)*:

$$u_n(r) = \frac{G_n a^2}{i\mu\alpha_n^2}\left[1 - \frac{J_0\left(i^{3/2}\alpha_n r/a\right)}{J_0\left(i^{3/2}\alpha_n\right)}\right] \quad (n \geq 1), \tag{1.19}$$

where

$$\alpha_n^2 = \rho n \omega a^2 / \mu. \tag{1.20}$$

$$\alpha^2 = \rho \omega a^2 / \mu \ (\equiv \alpha_1) \tag{1.21}$$

is the Womersley parameter.

For details of Bessel functions, see e.g. I.N. Sneddon, "Special Functions of Mathematical Physics and Chemistry", 3rd edition, Longman, pp. 130—132, which gives

$$J_0(i^{3/2}x) = I_0(i^{1/2}x) = \text{ber}\,(x) + i\,\text{bei}\,(x).$$

Ber and bei are known as Kelvin (or Thompson) functions (see Figure 1.10).

$$\text{ber}\,(x) = \sum_{s=0}^{\infty}(-1)^s(x/2)^{4s}/(2s!)^2, \quad \text{bei}\,(x) = \sum_{s=0}^{\infty}(-1)^s(x/2)^{4s+2}/(2s+1)!^2.$$
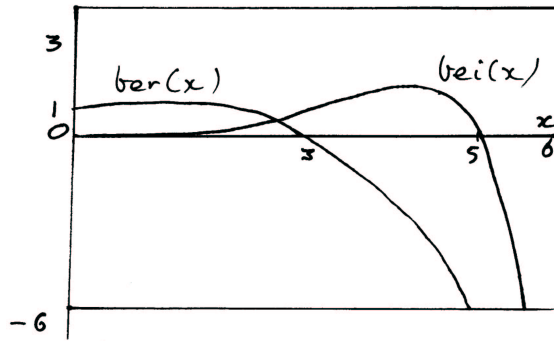

Figure 1.10: Sketch of the Kelvin functions.

What does the Womersley parameter measure?

(i) $\alpha^2 = O\left(\left[\dfrac{\partial u}{\partial t}\right] \Big/ \left[\nu\dfrac{\partial^2 u}{\partial r^2}\right]\right)$ = an unsteady Reynolds number.

(ii) $\alpha^2 = \left(a^2/\nu\right)/\left(1/\omega\right) \propto \dfrac{\text{viscous diffusion time}}{\text{period}}$ = frequency parameter.

For fluids of small viscosity, so that $\alpha_n \gg 1$, $(1.17) - (1.20)$ show that

$$u \sim \frac{G_0}{4\mu}(a^2 - r^2) + \frac{a^2}{\mu}\sum_{n=1}^{\infty}\frac{G_n}{\alpha_n^2}\sin n\omega t$$

$$-\frac{a^2}{\mu}\left(\frac{a}{r}\right)^{1/2}\sum_{n=1}^{\infty}\frac{G_n}{\alpha_n^2}e^{-\alpha_n(1-r/a)/\sqrt{2}}\sin\left[n\omega t - \alpha_n(1-r/a)/\sqrt{2}\right].$$

using the asymptotic behaviour of J_0.

This shows that when $\alpha_n \gg 1$, the flow consists of Poiseuille flow upon which is superimposed an unsteady core flow surrounded by a boundary layer of thickness $0(\alpha_n^{-1})$.

(iii) $\alpha = \dfrac{a}{\sqrt{\nu/\omega}} = \dfrac{\text{radius}}{\text{stokes b.l. thickness}}$ (Exercise).

If α is small, then taking the limits of the Bessel's functions, we find that $|u_n| \ll 1$ for $n \geq 1$ and the u_0 - terms give quasi-steady Poiseuille flow. Interpretation (iii) shows that the boundary layers fill the tube.

If α is large, then (iii) shows that the boundary layers are thin and (ii) shows that vorticity ($\boldsymbol{\omega} = \boldsymbol{\nabla} \times \mathbf{u}$) does not have time to diffuse across the tube before the flow reverses.

Experiments in which the pressure gradient waveform and the flow rate Q(t) were measured, show that this theory is successful in explaining the differences between the waveforms.

The flow rate $Q(t) = \int_0^a u(r)\, 2\pi r\, dr$ and using (1.19)

$$Q(t) = \pi a^2 \left\{ \frac{G_0 a^2}{8\mu} + \frac{a^2}{i\mu} \sum_1^\infty \frac{G_n}{\alpha_n^2} \left[1 - F(\alpha_n)\right] e^{in\omega t} \right\}, \qquad (1.22)$$

where

$$F(\alpha_n) \quad = \quad 2J_1(i^{3/2}\alpha_n)/i^{3/2}\alpha \ \ J_0(i^{3/2}\alpha_n)$$

$$\longrightarrow \quad \begin{cases} 1 - \dfrac{i\alpha^2}{8} & \text{as} \quad \alpha \longrightarrow 0 \ \ (\text{good for } \alpha < 4) \\[3mm] \dfrac{2}{i^{1/2}\alpha}\left(1 + \dfrac{1}{2\alpha}\right) & \text{as} \quad \alpha \longrightarrow \infty \ \ (\text{good for } \alpha > 4). \end{cases}$$

$$(1.23)$$

1.5   Nonlinear theory

The governing equations (1.1) — (1.3) are hyperbolic so we expect to be able to use the ideas of Riemann invariants, characteristics and shock waves.

We begin by rewriting (1.1) — (1.3) as

$$A_t + Au_x + uA_x = 0 \qquad (1.24)$$

and

$$u_t + uu_x + \left(c^2/A\right) A_x = 0, \qquad (1.25)$$

where

$$c^2(A) = AP'(A)/\rho \qquad (1.26)$$

which is <u>not</u> constant. Adding $\pm c/A$ times (1.24) to (1.25) gives

$$\left(\frac{\partial}{\partial t} + (u \pm c)\frac{\partial}{\partial x}\right)\left[u \pm \int_{A_0}^A \frac{c}{A^*}\, dA^*\right] = 0. \qquad (1.27)$$

$$\left(\text{Note that} \ \ \frac{\partial}{\partial t}\int_{A_0}^{A(x,t)} g(A^*)\, dA^* = g(A)\frac{\partial A}{\partial t} \ \ \text{etc.}\right)$$

Compare $\partial_t + (u \pm c)\partial_c$ with $D/Dt \equiv \partial_t + u\partial_x$ in 1-D fluid dynamics:

if $(\partial_t + u\partial_x)f = 0$, it means that the rate of change of f for a fluid particle moving with speed u is zero.

Thus, from (1.27) we have that the Riemann invariants

$$R_\pm = u \pm \int_{A_0}^A \frac{c}{A^*} \, dA^* \tag{1.28}$$

are constant on the characteristics, $C_\pm$, given by

$$C_\pm : \frac{dx}{dt} = u \pm c, \tag{1.29}$$

and so nonlinear waves propagate in the $\pm$ x-direction with variable speeds, $u \pm c$.

1.5.1 Shock formation

Propagation speeds are not uniform in general so characteristics can run together and form discontinuities or shocks.

Consider the situation in Figure 1.11 where blood is ejected from the left ventricle with velocity

$$U(t) \begin{cases} \geq 0 & \text{at } x = 0 \quad \text{for } t \geq 0 \\ = 0 & \text{at } x = 0 \quad \text{for } t < 0. \end{cases}$$
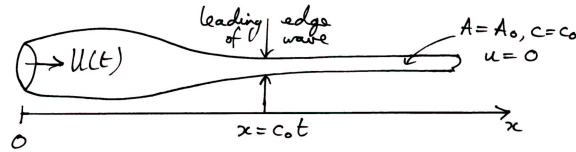

Figure 1.11: Pulse wave moving into undisturbed fluid.

The front of the pulse wave is moving into undisturbed fluid for which $c = c_0$ and so it propagates with speed c_0 (unless a shock forms at the front). This implies that

$$A = A_0, \quad c = c_0 \quad \text{and} \quad u = 0 \quad \text{for} \quad x > c_0 t.$$

Define $V(c) \equiv \int_{A_0}^A \frac{c(A^*)}{A^*} \, dA^*$, then $V(c_0) = 0 \, (\Longleftarrow A = A_0 \text{ when } c = c_0)$.
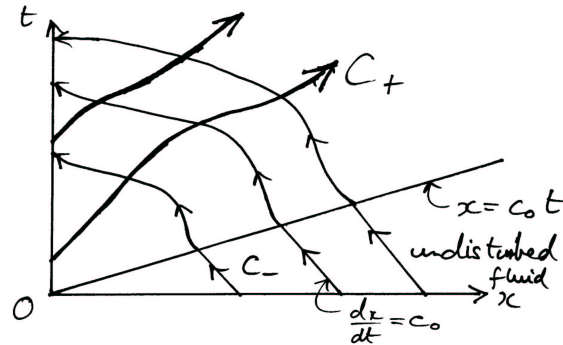
Figure 1.12: The characteristics for the propagation of the pulse wave.

We can draw an (x, t) phase diagram (Figure 1.12) to show the characteristics.

We know that $R_{\pm}$ = constant on $dx/dt = u \pm c$.

In $x > c_0 t$, $u = 0$, $c = c_0$ and

$$R_- = 0 \quad \Longrightarrow \quad u = V(c)$$

on all C_- characteristics originating in $x > c_0 t$, even when they move into the disturbed region.

$$\therefore \quad \underline{u = V(c), \text{ throughout the fluid.}}$$

Consider the C_+ characteristics in $x < c_0 t$.

$u = V(c)$ everywhere $\Longrightarrow$ $R_+ \equiv u + V(c) = 2u$
$\Longrightarrow$ u = constant everywhere $\Longrightarrow$ c = constant everywhere $(\because u = V(c))$
$\Longrightarrow$ $\underline{C_+ \text{characteristics are straight lines,}}$

although they can have different slopes.

Shocks form where the characteristics intersect and we can calculate when this will first happen (Figure 1.13).

A typical C_+ characteristic starting at $t = \tau$ from $x = 0$ is

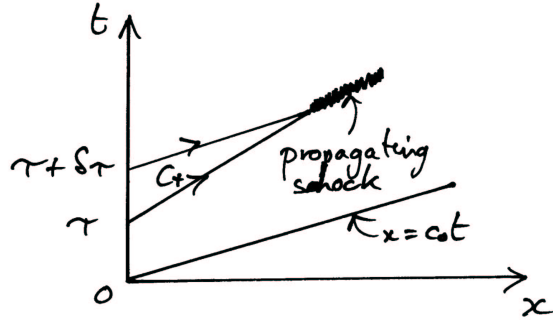$$x = [U(\tau) + c(U(\tau)] (t - \tau) \tag{1.30}$$

Figure 1.13: Shock formation.

with neighbouring characteristic

$$x = [U(\tau + \delta\tau) + c(U(\tau + \delta\tau))]\,(t - \tau - \delta\tau). \tag{1.31}$$

Equating (1.30) and (1.31) and letting $\delta\tau \longrightarrow 0$ tells us that the characteristics meet at time

$$\underline{t_s = \tau + F(U(\tau))/\dot{u}(\tau)F'(U(\tau))}, \tag{1.32}$$

where

$$F(U(\tau)) \equiv U(\tau) + c(U(\tau)). \tag{1.33}$$

A shock will first form when $t_s(\tau)$ has a minimum.

Example

Take $P(A) = \rho c_0^2 A^2/2A_0^2 + \text{constant}$

$$\text{and}\quad U(t) = \begin{cases} U_0\left[1 - (1 - t/t_0)^2\right] & ,\quad 0 \le t \le 2t_0, \\ 0 & ,\quad t < 0 \ \text{and}\ t > 2t_0 \end{cases}$$

(see Figure 1.14).
Then $c = c_0 A/A_0$, $V(c) = c_0(A - A_0)/A_0 = c - c_0$ and therefore $F = 2U + c_0$.
Equation (1.32) gives

$$t_s(\tau) = \tau + (c_0 + 2U)\,t_0^2/4U_0(t_0 - \tau),$$

which has a minimum at $\tau = 0$, so that the first shock appears when

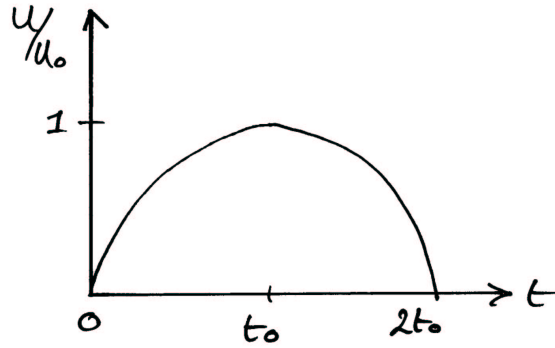$$\underline{t_s = c_0\ t_0/4U_0} \quad \text{at} \quad \underline{x_s = c_0^2\ t_0/4U_0}.$$

Figure 1.14: Ejection velocity.

For typical physiological conditions in man, x_s is longer than the aorta and a shock would not be expected to form. However, when there is "aortic valve incompetence", the heart compensates by ejected a greater volume of blood and clinicians report a "pistol-shot pulse", which is likely to correspond to the formation of a shock.